Research on explosive dust space ventilation scheme based on CFD simulation

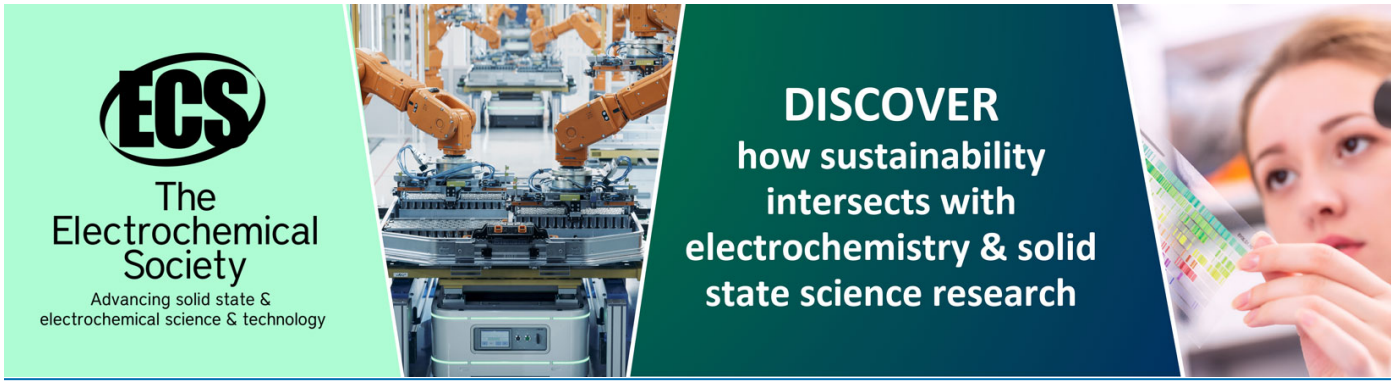

Research on explosive dust space ventilation scheme based on CFD simulation

D Wang, Q Jing, X M Qian, M Q Yuan*, and S Q Liu

State Key Laboratory of Explosion Science and Technology, Beijing Institute of Technology, Beijing 100081, China

wangdan0226@foxmail.com

Abstract. Aluminum powder with high explosive sensitivity, strong detonation performance and low price has become the first choice fuel for fuel air explosives. Design three types of exhaust schemes for specific powder operation spaces, and use CFD simulation technology to study the flow field and dust removal characteristics of the three schemes. The results show that the bottom ventilation scheme has the best dust removal effect, the characteristic time of dust removal is 9.4s, and the maximum dust concentration is 85g/m^3. And the characteristic flow field range of the bottom exhaust scheme is the smallest (4.12m×3.05m), which indicates bottom scheme has the least disturbance to the spatial flow field, so this scheme should be selected for ventilation and dust removal design. In addition, the function relationship between the wind pressure and the characteristic dust removal time is obtained by setting different wind pressures, which provides a basis for the design of the graded ventilation dust removal side according to the design.

1. Introduction

Aluminum powder is not only an important industrial raw material, but also has a wide range of military application backgrounds due to its high combustion heat value. In addition, aluminum powder is prone to detonation in the air, and is relatively cheap, so it has become the fuel of choice for fuel air explosives(FAE). The investigation found that there is a large amount of dust dispersed during the normal operation in the aluminum powder operation workshop, which will cause great hazards of explosion and occupational health. Therefore, fan ventilation should be turned on during normal operation to limit the dust concentration in the operating space to a safe concentration range. In addition, due to personnel's misoperation or mechanical failure, temporary dust concentration will suddenly increase in the space. Conventional ventilation cannot quickly reduce the dust concentration. At this time, a more powerful fan is required to enhance ventilation.

There are lots of research has been done about the ventilation and dust removal characteristics of tunnel construction, coal mine tunnels and dust production workshops. Hall [1] and Hodkinson [2] obtained the optimal dust extraction wind speed and gas-solid separation technology through experiments. S.L. Soo [3] proposed a gas-solid two-phase flow model. Nakayama Shinsuke, Ueno Kenichi and P.J.Witt et al. [4] studied the distribution of wind flow in the tunnel by experiments studies and dynamic fluid models, respectively, and they predicted the trajectory of wind flow through computer simulation. Jun Wang et al. [5], American scientist, found that there is a momentum transfer relationship between particles and gas. Descamps et al. [6] studied the relationship between coal dust

concentration and particle size distribution in coal rocks through experiments. Ge Wenchang [7] in China using a specific tunnel as the background, develops the overall design of the tunnel dust removal vehicle according to the tunnel dust generation mechanism and ventilation and dust removal requirements. The main performance parameters such as the processing air volume, filtering wind speed, and filtering area of the dust collector were determined by calculation, and the reasonable selection and layout were based on the parameters. Dai Jiangjiao [8] analyzed the influence of the parameters of the air duct on the dust removal efficiency of an actual tunneling ventilation system through experiments. Zhang Xiaoliang et al. [9] summarized and discussed the selection of dust removal equipment, equipment explosion-proof selection and dust removal system in industrial workshops based on the classification of dust properties and explosion risk areas, combined with combustible dust characteristic parameters and ventilation parameters.

At present, CFD simulation technology has been widely used in the study of gas-dust two-phase flow. The law of dust movement in the flow field can be predicted by numerical simulation, which has a significant effect on solving practical engineering problems. Wang Xiaozhen, Niu We, and other scholars [10] by modeling(4m×3m), obtained the wind speed range and air duct layout parameters for the best dust removal effect of press-in ventilation. Jiang Zhongan et al. [11]~[14] established a 3D model of a coal mine heading roadway. The steady-state solution method was used to simulate the dust distribution law under the ventilation conditions such as press-in and mixed pumping. They compared the effects of the ratio of the suction pressure air volume, the location of the suction pressure air duct, and the air curtain on the dust concentration distribution range and the particle size deposition rule, and analyzed the reasonable arrangement of the suction pressure ratio of the air flow and the position of the air cylinder. Based on the comparison between the analysis results and the measured data, they proposed a guidance for dust removal methods, and analyzed the dust removal effect.

In this paper, three ventilation schemes are designed, for specific aluminum powder operation workshops, which are upper exhaust, side exhaust and bottom exhaust. The CFD simulation technology was used to study the flow field and dust removal characteristics of the three schemes to obtain the optimal exhaust mode. By setting different wind pressures to study the relationship between wind pressure and dust removal time, it can provide a basis for designing a graded ventilation dust removal party as designed.

2. Computational models

2.1. Governing equations of gas and discrete phase

The ventilation and dust removal process studied in this paper is a gas-dust two-phase flow. The sparse second phase in the CFD simulation is considered to be a discrete phase distributed in the continuous phase. Dust diffusion involves turbulence, gas-solid two-phase heat and mass transfer, etc. Therefore, the basic N-S governing equations (1)~(5), turbulent flow equations (6)~(9), and discrete phase force equations (10)~(14) must be observed in the calculation. The finite volume method is used to solve the N-S equation, and the pressure-based SIMPLE solver is used for numerical solution.

Mass conservation equation:

$$\frac{\partial \rho Y_k}{\partial \mathrm{t}} + \frac{\partial_{\rho u_i}}{\partial x_i}\left(\rho(u_i + V_{k,i})Y_k\right) = \dot{\omega}_k \tag{1}$$

Momentum conservation equation:

$$\frac{\partial}{\partial \mathrm{t}}(\rho u_i) + \frac{\partial}{\partial x_i}\left(\rho u_i u_j\right) = -\frac{\partial p}{\partial x_j} + \frac{\partial \tau_{ij}}{\partial x_i} + \rho \sum_{k=1}^{N} Y_k f_{k,j} = \frac{\partial \sigma_{ij}}{\partial x_i} + \rho \sum_{k=1}^{N} Y_k f_{k,j} \tag{2}$$

$$\tau_{ij} = -\frac{2}{3}\mu \frac{\partial u_k}{\partial x_k}\delta_{ij} + \mu\left(\frac{\partial u_i}{\partial x_j} + \frac{\partial u_j}{\partial x_i}\right) \tag{3}$$

$$\sigma_{ij} = \tau_{ij} - p\delta_{ij} = -p\delta_{ij} - \frac{2}{3}\mu \frac{\partial u_k}{\partial x_k}\delta_{ij} + \mu\left(\frac{\partial u_i}{\partial x_j} + \frac{\partial u_j}{\partial x_i}\right) \tag{4}$$

Energy conservation equation

$$\frac{\partial \rho E}{\partial t}+\frac{\partial}{\partial x_i}(\rho u_i E)=\dot{\omega}T+\frac{\partial}{\partial x_i}\left(\lambda\frac{\partial T}{\partial x_i}\right)-\frac{\partial}{\partial x_i}(\rho\sum_{k=1}^{N}h_{s,k}Y_kV_{k,i})+\sigma_{ij}\frac{\partial u_i}{\partial x_j}+\dot{Q}+\rho\sum_{k=1}^{N}Y_kf_{k,i}(u_i+V_{k,i}) \quad (5)$$

The RNG standard k-ε model for continuous phase is as follow:

$$\frac{\partial}{\partial t}(\bar{\rho}k)+\frac{\partial}{\partial x_i}(\bar{\rho}\tilde{u}_ik)=\frac{\partial}{\partial x_i}\left[\left(\mu+\frac{\mu_t}{\sigma_k}\right)\frac{\partial k}{\partial x_i}\right]+P_k-\bar{\rho}\varepsilon \quad (6)$$

$$\frac{\partial}{\partial t}(\bar{\rho}\varepsilon)+\frac{\partial}{\partial x_i}(\bar{\rho}\tilde{u}_i\varepsilon)=\frac{\partial}{\partial x_i}\left[\left(\mu+\frac{\mu_t}{\sigma_\varepsilon}\right)\frac{\partial \varepsilon}{\partial x_i}\right]+C_{\varepsilon1}\frac{\varepsilon}{k}P_k-C_{\varepsilon2}\bar{\rho}\frac{\varepsilon^2}{k} \quad (7)$$

Where:

$$\mu_t=\bar{\rho}C_\mu\frac{k^2}{\varepsilon} \quad (8)$$

$$P_k=-\bar{\rho}\widetilde{u''_iu''}_j\frac{\partial \tilde{u}_i}{\partial x_j} \quad (9)$$

And the model constant have the default value:

$$C_\mu=0.09;\ \ \sigma_k=1.0;\ \ \sigma_\varepsilon=1.3;\ \ C_{\varepsilon1}=1.44;\ \ C_{\varepsilon2}=1.92$$

The discrete phase model (DPM) opted for the particulate phase predicts the trajectory of a discrete phase particle by integrating the force balance on the particle, which is written in a Lagrangian reference frame. The force balance equates the particle inertia with the forces acting on the particle, and can be written (for the x direction in Cartesian coordinates) as:

$$\frac{\mathrm{d}u_p}{\mathrm{d}t}=F_D(u-u_p)+\frac{g_x(\rho_p-\rho)}{\rho_p}+F_x \quad (10)$$

Where:

$$F_D=\frac{18\mu}{\rho_p d_p^{\,2}}\frac{C_D\,\mathrm{Re}}{24} \quad (11)$$

$$\mathrm{Re}=\frac{\rho_p d_p\left|u_p-u\right|}{\mu} \quad (12)$$

$$\begin{cases} C_D=\dfrac{24}{\mathrm{Re}}(1+0.15\,\mathrm{Re}^{0.687})(\mathrm{Re}<800) \\ C_D=\dfrac{19.65}{\mathrm{Re}^{0.633}}(5<\mathrm{Re}<100) \end{cases} \quad (13)$$

$$F_x=\frac{1}{2}\frac{\rho}{\rho_p}\frac{d}{dt}(u_p-u) \quad (14)$$

2.2. Hypothesis of physical and chemical models

The gas-particle multiphase flow studied in this paper is based on the following basic assumptions:

(1) Assuming that the aluminum powder particles are spherical particles of equal particle size;

(2) Ignore the energy loss due to wall friction and heat conduction of the pipe wall;

(3) It is assumed that the collision between the particle phase and the avoidance is an inelastic collision, and the momentum of the falling dust is reduced to zero;

(4) Consider the interaction between the gas phase and the particle phase during the diffusion process, and ignore the fragmentation effects caused by the collision between the particles.

2.3. Conditions and parameters

The air inlet of the aluminum powder workshop studied in this paper is located on the bottom surface, and a 3m (length)×3m (width)×2m (height) cuboid space is set at the corner of the workshop as the dust operation space. A uniform dust cloud is sprayed in the operation space and a concentration sensor is arranged. The cross section of the exhaust duct is a square of 0.5m×0.5m. Three ventilation schemes are designed, which are three modes of upper exhaust, bottom exhaust and side exhaust, as

shown in figure 1. Seventeen sensors are arranged in the operating space to monitor the change of dust concentration during ventilation. The sensor arrangement is shown in figure 2. The four monitoring points numbered 6-9 are used to monitor the change of dust concentration near the ground to characterize the dust deposition, and the remaining monitoring points are used to monitor the dust concentration in space.

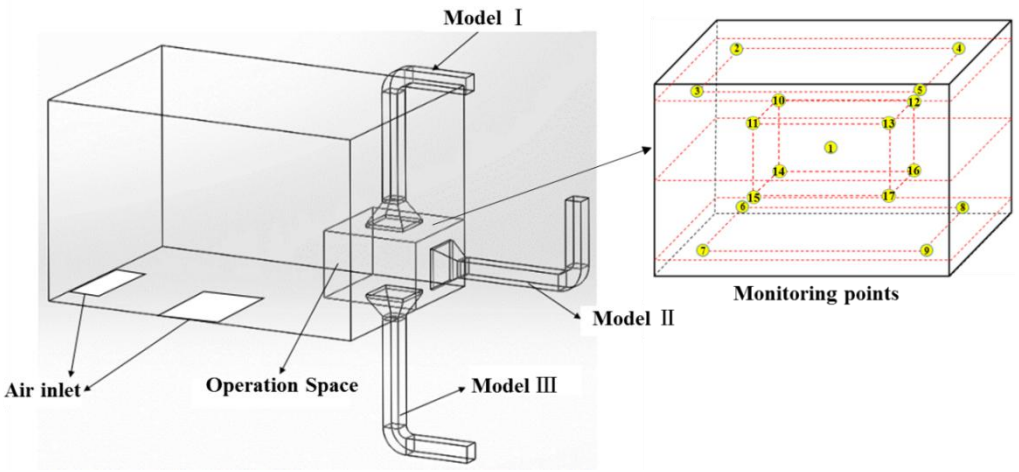

Figure 1. Ventilation scheme and monitoring points.

Table 1. Mesh models.

Model	Scheme	Grid Number	Grid quality
Model Ⅰ	Upper ventilation	287462	0.83
Model Ⅱ	Side ventilation	280501	0.92
Model Ⅲ	Bottom ventilation	282105	0.92

The three scheme models are divided into meshes, all of which use a hexahedron structured mesh, and the operation space and the exhaust duct are grid-encrypted. Considering the accuracy of the calculation results and the computing hardware conditions comprehensively, the number and quality of the final divided grids are shown in table 1. The quality of the grid meets the accuracy requirements of simulation calculations.

In this paper, the density, planar particle size and thickness of the flake aluminum powder used in the workshop selected is 2700kg/m^3, 50μm, and about 1μm respectively. In simulation, it is equivalent to spherical aluminum powder particles with a diameter of 15.5μm. The lower explosion limit of the aluminum powder with this particle diameter was 60 g/m^3. Therefore, set the initial dispersion concentration in the operating space to 60 g/m^3 (100% LEL). By setting the outlet negative pressure simulation fan, the wind pressure range is set to -20Pa ~ -300Pa to simulate different power fans. The safety critical concentration of ventilation and dust removal is set to 6g/m^3 (10% LEL), in other words, the dust concentration in the operating space has dropped to this concentration and reached the safety standard. The meshing and initial dust dispersion of the three schemes are shown in figure 2.

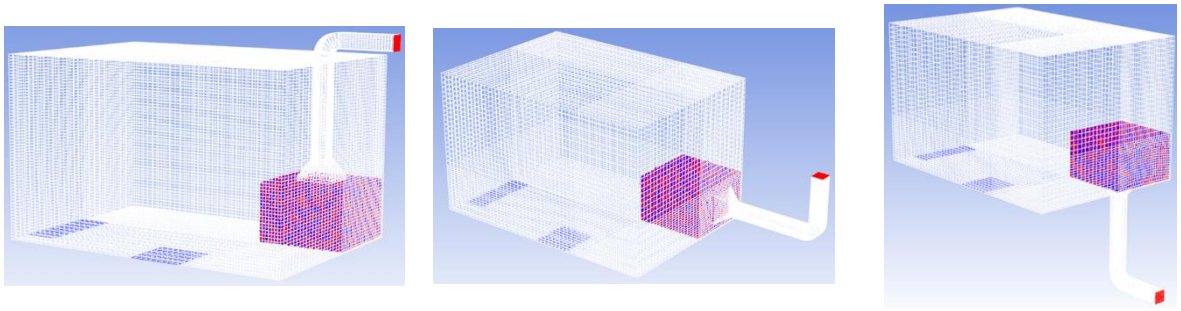

(a) (b) (c)

Figure 2. Mesh and initial state of the three schemes.

3. Results and discussion

3.1. Wind pressure and space flow field

To study the ventilation effect of the workshop, the relationship between the fan wind pressure and the exhaust pipe exhaust flow in the experimental workshop should be studied first. Figure 3 shows the time history of the air duct flow corresponding to different outlet air pressures. As the outlet air pressure increases, it takes longer to stabilize the exhaust air flow. This article studies the dust removal process in the stable phase.

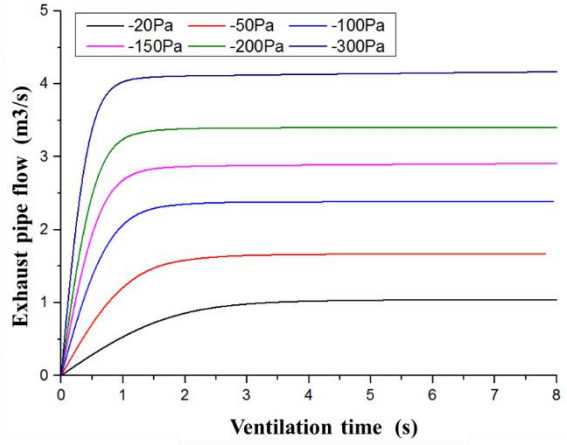

Figure 3. Time history of flow at different wind pressures.

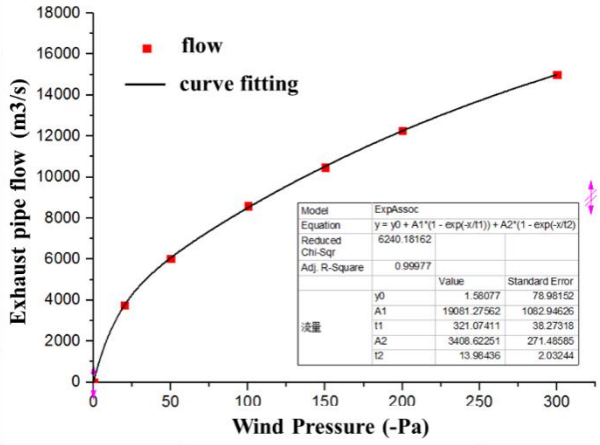

Figure 4. Curve fitting of wind pressure and flow.

Figure 4 shows the relationship between the outlet wind pressure and the steady-state flow rate, and the data points are fitted to the equation (15). The fitting similarity is 0.99977, so the fan that meets the wind pressure requirements can be selected according to the required flow.

$$Q = 1.58077 + 19081.27562\left(1 - e^{-\frac{P}{321.07411}}\right) + 3406.62251\left(1 - e^{-\frac{P}{13.98436}}\right) \quad (15)$$

The dust operation workshop usually chooses a 15kW power fan with a flow rate of about 6500m^3/h and a corresponding outlet wind pressure of about -100Pa. It is found from figure 3 that the flow is stable after the fan is turned on for 4 seconds. Therefore, the simulation of the dust removal process is set to a wind pressure of -100Pa, and after 4s of ventilation, a uniform dust cloud is charged to compare the exhaust and dust removal effects.

The flow field distribution of the longitudinal section of the air ducts for the three exhaust schemes is shown in figure 5. In the upper exhaust scheme, the maximum velocity is 13.5m/s, and the

maximum velocity in the workshop is 0.5m/s. Then, the maximum velocity in the duct of the side exhaust scheme is 13.5m/s, and the maximum velocity in the workshop is 0.5m/s. The maximum air velocity in the duct of the bottom exhaust scheme is 13.5m/s, and the maximum velocity in the workshop is 0.5m/s.

In this paper, the 0.075m/s velocity is defined as the boundary velocity of the characteristic flow field, which is used to compare the spatial range of the turbulent disturbance caused by different exhaust schemes on the spatial flow field. As shown in Figure 5, the size of the characteristic flow field region of the upper exhaust scheme is 5.63m×3.44m. The characteristic flow field area size of the side exhaust scheme is 4.17m×3.25m. And, the characteristic flow field area size of the lower exhaust scheme is 4.12m×3.05m.

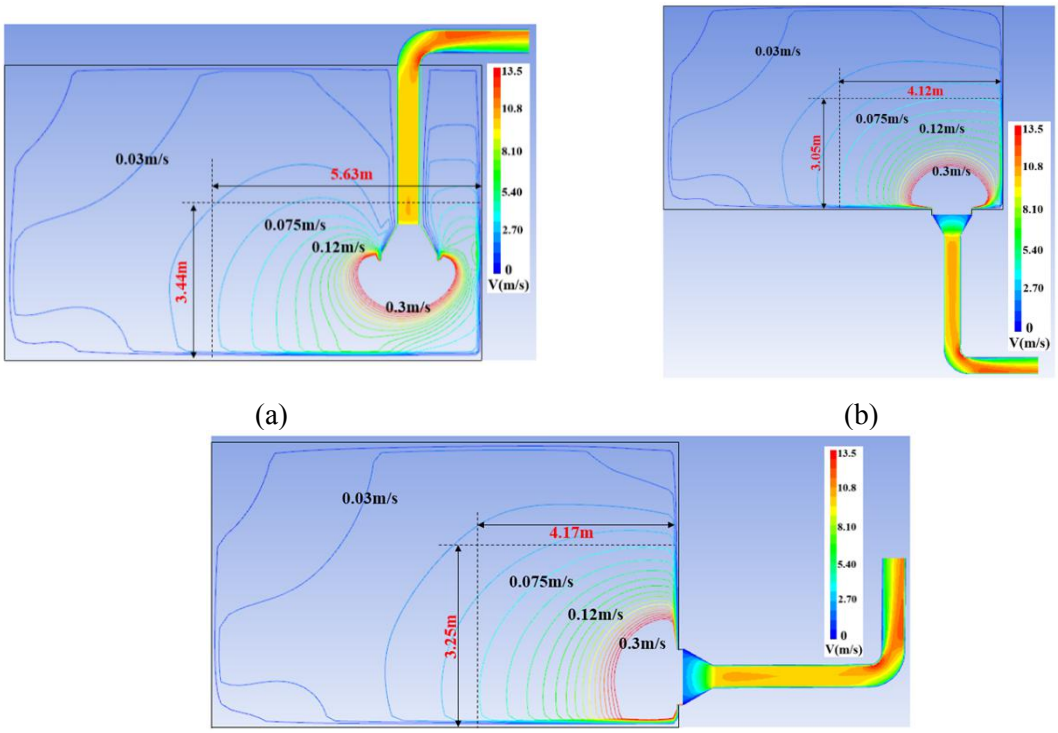

Figure 5. Flow field distribution in different scenarios.

3.2. Dust removal effect of three schemes

When the flow field is stabilized, the operation space is filled with a uniform dust cloud. The initial dust cloud concentration distribution of the three solutions is shown in figure 6, and the initial concentration is 60g/m^3.

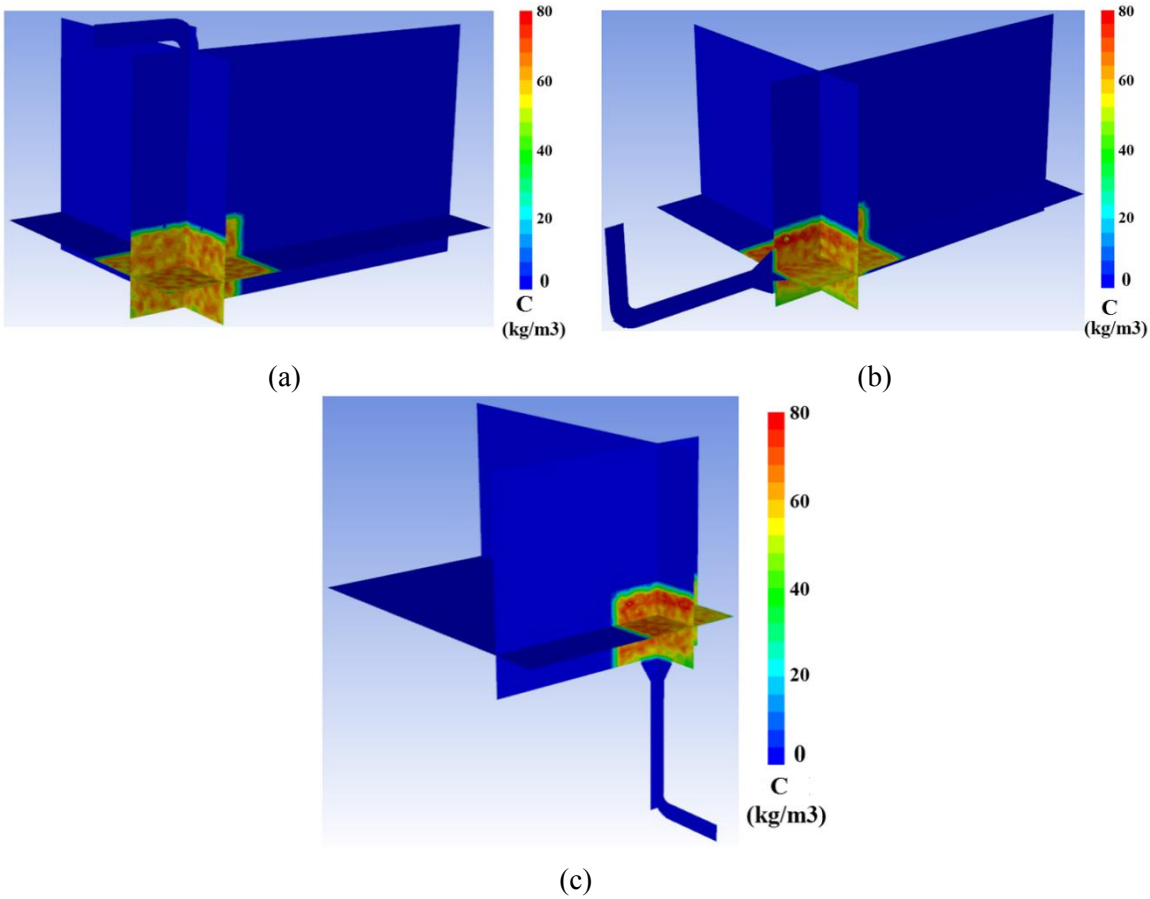

Figure 6. Initial dust concentrate contours.

The concentration change of the monitoring points in the operating space can represent the dust removal effect. The time-history change curve of the dust concentration measured by the 14 sensors in the operating space is shown in figure 7. The 6 g/m^3 (10% LEL) is defined as the safe concentration limit, so for the upper exhaust scheme, the time for the concentration of all points to fall to the safe limit time is 24s, of which the first 4s is the ventilation time, so the characteristic dust removal time is 20s. Within the operating space, the maximum concentration is 220g/m^3. Similarly, the characteristic dust removal time of the side exhaust scheme is 25s, and the maximum concentration in the operating space is 240g/m^3. The characteristic dust removal time of the bottom exhaust scheme is 9.4s, and the maximum concentration in the operating space is 85g/m^3.

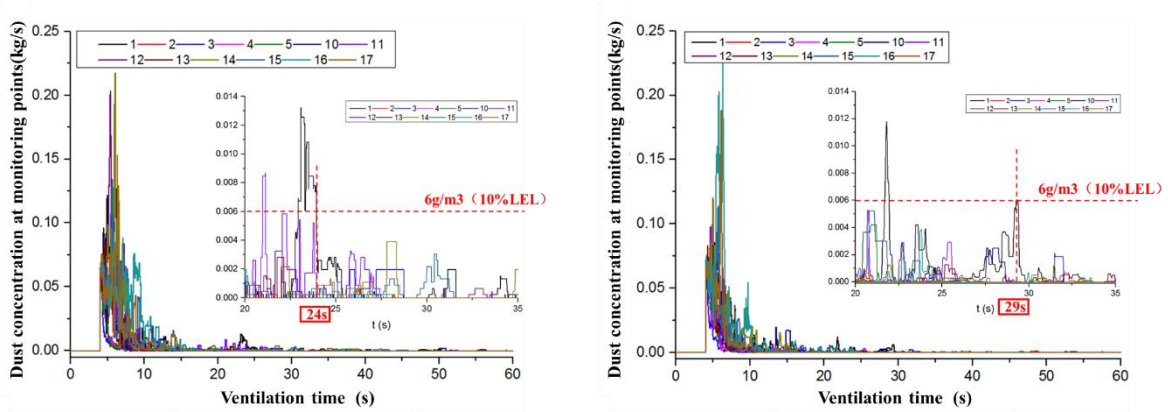

(a) (b)

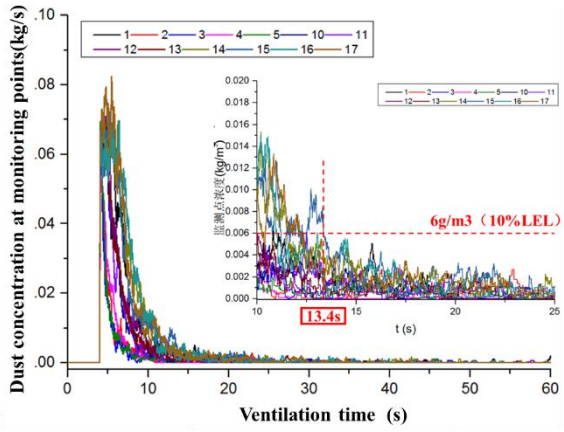

(c)

Figure 7. Dust concentration change in operating space.

The aluminum powder used in the workshop is sheet-mounted aluminum powder, which will hardly rebound after contacting the ground, so a non-elastic collision model is used to handle the momentum change during the contact between the aluminum powder and the ground. Due to gravity and the collision and accumulation of dust particles, dust accumulation will be formed on the ground during the dust removal process. The concentration change curves of the four sensors near the ground are shown in figure 8. The dust concentration in the upper exhaust scheme decreased rapidly in the initial stage, and dust accumulation occurred within 15s to 32s, with the highest concentration reaching 550g/m^3. The side exhaust scheme collects dust at the 9th measurement point within 10s~30s, and the highest concentration can reach 2100g/m^3. At the monitoring point 8 of the bottom exhaust scheme, obvious dust accumulation occurred, the highest concentration could reach 110g/m^3, and the concentration began to decrease after 13s. The dust migration process caused small concentrations of high values at other monitoring points.

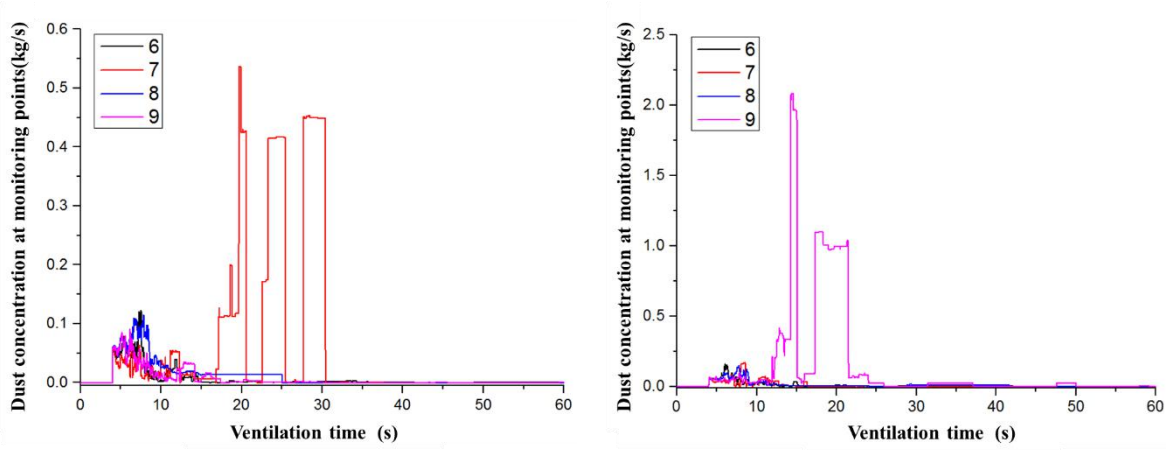

(a) (b)

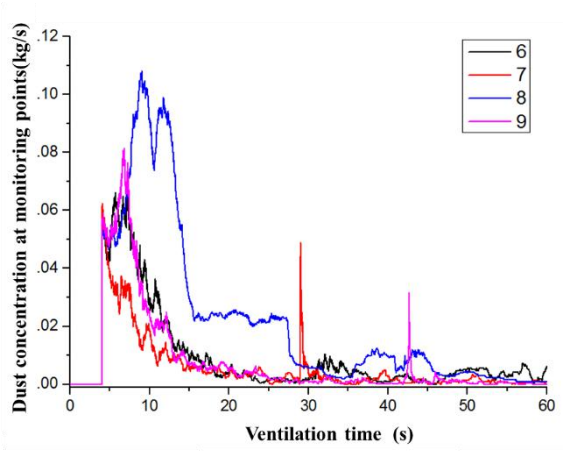

(c)

Figure 8. Dust concentration change near the ground.

3.3. Optimized ventilation scheme

Considering the flow field distribution and dust removal process of the three schemes, the characteristic parameters are summarized in table 2. It can be seen that the bottom exhaust mode has obvious advantages over the other two schemes. The main reason is that the air inlet of this workshop is located at the bottom. The lower exhaust method can control the effective flow field in a lower space, and the effect of gravity is favorable for the dust sedimentation to be discharged from below. Therefore, the bottom exhaust method should be selected for efficient ventilation.

Table2. Effect comparison of three dust removal schemes.

Model	Model Ⅰ	Model Ⅱ	Model Ⅲ
Scheme	Upper ventilation	Side ventilation	Bottom ventilation
Characteristic flow field size	5.63m×3.44m	4.17m×3.25m	4.12m×3.05m
Characteristic dust removal time of operating space	20s	25s	9.4s
Maximum concentration in operating space	220g/m^3	240g/m^3	85g/m^3
Maximum concentration near the ground	550g/m^3	2100g/m^3	110 g/m^3

There is always dust dispersion in the aluminum powder operation workshop. During normal operation, the fan needs to be turned on for concentration control to control the dust concentration in the space within a safe range. When there is a malfunction or mechanical failure in the workshop, a temporary dust concentration will suddenly increase. At this time, a more efficient ventilation mode needs to be turned on to decrease the concentration quickly. Based on this, a variable frequency fan is selected for ventilation and dust removal, and a hierarchical ventilation mode with different levels of ventilation effects is designed. Set different outlet negative pressures to get the characteristic dust removal time under the conditions of -20Pa ~ -300Pa.

$$t = 260.2355 \times Q^{-0.36446} \tag{16}$$

A functional relationship between the characteristic dust removal time and its corresponding exhaust air flow was fitted. The fitting result is shown in Figure 9, and the fitting relation is Equation (16). The fitting degree of the fitting result is 0.96834. According to this formula, a fan that meets the

requirements of dust removal can be selected according to the requirement of hierarchical early warning.

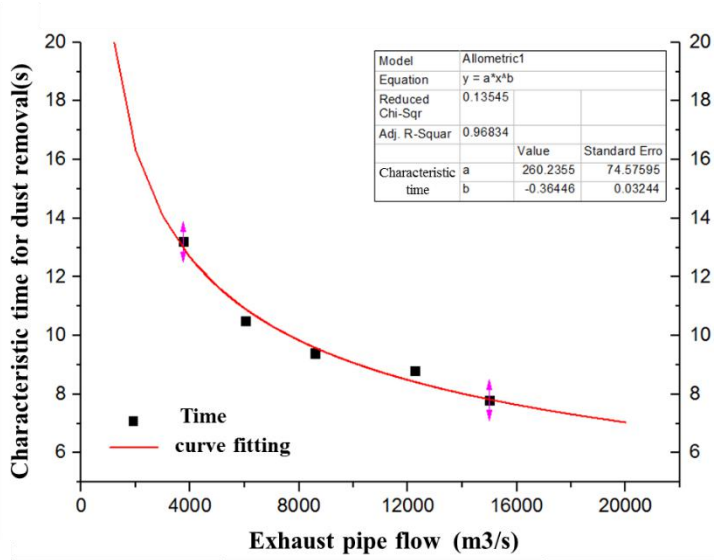

Figure 9. Initial dust concentrate contours

4. Conclusion

In this paper, three ventilation schemes are designed for specific aluminum powder operation workshops, which are upper exhaust, side exhaust and bottom exhaust respectively. The CFD simulation technology was used to study the flow field and dust removal characteristics of the three schemes. The study found that when the initial dust concentration was 60g/m^3(100% LEL), the dust removal characteristic time of the upper exhaust scheme was 20s, and the maximum dust concentration was 220g/m^3. Then, the dust extraction characteristic time of the side exhaust scheme was 25s, and the maximum dust concentration was 240g/m^3. In addition, the characteristic time of dust removal at the bottom exhaust scheme is 9.4s, and the maximum dust concentration is 85g/m^3, so the bottom exhaust scheme has the highest dust removal efficiency. And the characteristic flow field range of the lower exhaust scheme is the smallest(4.12m×3.05m), which indicates the bottom scheme has the least disturbance to the spatial flow field, so this scheme should be selected for ventilation and dust removal design. In addition, the function relationship between the wind pressure and the characteristic dust removal time is obtained by setting different wind pressures, providing a basis for the design of the graded ventilation dust removal side according to the design.

Acknowledgements

This article was supported by the National Key Research and Development Program of China (Grant No. 2017YFC0804700) and the National Natural Science Foundation of China (Grant No. 71861167002 and No. 5183000192).

References

[1] Hall D A 1957 *Trans. Inst. of Min. Eng.***117** 25-28
[2] Hodkinson J R 1957 *Trans. Inst. of Min. Eng*
[3] Guo L J 2002 *Two phase and multiphase fluid dynamics*(xi'an)
[4] Witt P J and Caret' K G 2002 *Appl. Math. Model.* **26** 297-309
[5] Wang J and Levy E K 2003 *Experimental Thermal & Fluid Science* **27** 845-53
[6] Descamps I, Harion J L and Baudoin B 2005 *Chemical Engineering &Proc.* **44** 159-166

[7] Ge W C 2018 *Simulation and optimization of flow field in filter cartridge dust collector for drilling and blasting method* (Chengdu: Southwest Jiaotong University)
[8] Dai J J 2017 *Study on flow field characteristics of ventilation system and dry dust collector in heading face* (Taiyuan:Taiyuan University of Technology)
[9] Zhang X L, He R, Song H J and Cao X G 2018 *Industrial Safety and Environmental Protection* **44** 52-55 + 71
[10] Wang X Z 2011 *Safety Science and Technology of China* 75-7
[11] Wang X Z, Jiang Z G and Liu Y 2006 *China Safety Science and Technology* **2** 24-8
[12] Yao H F, Deng Z G and Li J L 2014 *Coal Mining* 96-9
[13] Qin Y P, Zhang M M and Cui L J 2011 *Journal of University of Science and Technology Beijing* **33** 790-4
[14] Du C F, Wang H and Jiang Z G 2010 *Journal of Engineering Science* **32** 957-62